# Interpretation of water retention field measurements in relation to hysteresis phenomena

Davide Canone,[1] Stefano Ferraris,[1] Graham Sander,[2] and Randel Haverkamp[1]

[1] Knowledge of the soil water retention function is fundamental to quantifying the flow of water and dissolved contaminants in the vadose zone. This function is usually determined by fitting a particular model (see, for example, van Genuchten (1980) or Brooks-Corey (1964)) to observed retention points. Independent of the model chosen, interpretation and identification of the water retention parameters are subjective and prone to error, particularly as it is common that the hysteresis history in measured data points is unknown. Experimental data sets from three different field soils are used to clearly demonstrate how the lack of hysteresis knowledge can lead to an inconsistent and incorrect interpretation of the retention data, and therefore to the incorrect estimation of soil hydraulic parameters. By using a hysteresis model to interpret this same data set, it is easily shown that consistent and reliable estimates of soil retention parameters can be obtained. This is true for any physically based hysteresis model. The difficulty in reading water retention measurements may be evident when both drying and wetting data are measured. However, in practice, users are rarely aware of this problem since generally only one set of drying data is measured, making comparison impossible. Such erratic interpretation of water retention field data in the literature will be probably far more common than expected.

## 1. Introduction

[2] Describing and quantifying flow and transport in the vadose zone requires knowledge of the soil water retention function which relates soil water pressure head with volumetric soil water content, and the conductivity function which relates hydraulic conductivity with soil water content or pressure head. Here, we focus on the description of the water retention function.

[3] Many different equations have been proposed to parameterize water retention data [e.g., *Gardner*, 1958; *Brooks and Corey*, 1964; *Brutsaert*, 1966; *Haverkamp et al.*, 1977; *van Genuchten*, 1980; *Kosugi*, 1994; *Assouline et al.*, 1998]. We consider one of the most popular among them for this study, i.e., the van Genuchten equation:

$$\theta* \equiv \frac{\theta - \theta_r}{\theta_S - \theta_r} = \left[1 + \left(\frac{h}{h_g}\right)^n\right]^{-m}, \quad (1)$$

where $\theta*$ is the degree of saturation, $\theta$ is the volumetric soil water content [$L^3/L^3$], and $\theta_S$ and $\theta_r$ [$L^3/L^3$] are water content scaling parameters that denote the (maximum) saturated and (minimum) residual volumetric soil water

content, respectively. The soil water pressure head $h$ [L] is taken to be negative for unsaturated conditions and is expressed in centimeters of water. The parameter $h_g$ [L] is the van Genuchten pressure head scale parameter.

[4] Equation (1) contains two dimensionless shape parameters, $m$ [$-$] and $n$ [$-$] usually related through

$$m = 1 - \frac{k_m}{n} \text{ with } n > k_m, \quad (2)$$

where the parameter $k_m$ is referred to as the user index [*Haverkamp et al.*, 2005; *Leij et al.*, 2005]. Even though $k_m$ may take any positive value, integer values are often chosen in order to accommodate closed form analytical expressions selected by the user for the hydraulic conductivity. The user index $k_m = 1$ ($n > 1$) corresponds to the conductivity model of *Mualem* [1976] while $k_m = 2$ with $n > 2$ gives the conductivity model of *Burdine* [1953].

[5] The use of equations (1) and (2) for the description of water transfer processes, requires a priori determination of five unknown water retention system parameters, i.e., two shape parameters $m$ and $n$, and three scale parameters $\theta_S$, $\theta_r$ and $h_g$. Both shape parameters are strongly linked to the textural soil properties, whereas the scale parameters are related to soil structure [*Haverkamp et al.*, 2002a]. The parameters are generally estimated by fitting the water retention equation to measured $h(\theta)$ data points and should result in a unique parameter set for a particular retention function, independent of the choice of optimization method. It may also be necessary to impose constraints during the optimization of the system parameters to either ensure that

---

[1]Department of Economics and Agricultural, Forestry and Environmental Engineering, University of Turin, Grugliasco, Italy.
[2]Department of Civil and Building Engineering, Loughborough University, Loughborough, UK.

retention function reproduces the actual data, or to minimize the number of parameters. Classically, constraints are imposed on the shape parameter $m$ and the scale parameter $\theta_r$ [*van Genuchten et al.*, 1991].

[6] Using a prefixed value of $k_m$ (e.g., $k_m = 1$ or $k_m = 2$) the number of shape parameters is reduced to one (either $m$ or $n$) without affecting a priori the fitting abilities of the van Genuchten model (equation (1)) [*Leij et al.*, 1997]. The case of the scale parameter $\theta_r$ is more delicate. Conceptually, the residual water content may be associated with the immobile water held (by adsorptive forces) within in a dry soil profile in films on particle surfaces, in interstices between particles, and within soil pores. In practice however, its value is generally estimated by fitting the water retention equation to measured data points reducing $\theta_r$ to an empirical fitting parameter valid for the range of data points used. It may well give doubtful results when applied beyond this range of data points (e.g., for the simulation of evaporation). For this reason, various authors set its value equal to zero, $\theta_r = 0$ [e.g., *Kool et al.*, 1987; *van Genuchten et al.*, 1991; *Leij et al.*, 1996].

[7] In this study, the value of $\theta_r$ is related to the wetting and drying history prior to the measurement of the $h(\theta)$ data points in line with the hysteresis model of *Haverkamp et al.* [2002b]. Setting $\theta_r = 0$ for the main hysteresis loop, the scanning curves will have nonzero $\theta_r$-values. The nonzero $\theta_r$-value is then attributed to a wetting or drying curve of a higher scanning order rather than to the main wetting or drying curve. This eliminates $\theta_r$ as a soil characteristic parameter (at least for soils with unimodal behavior) to be estimated through fitting.

[8] Several conceptual and empirical models of varying complexity have been introduced in the literature to describe the hysteretic behavior of the water retention $\theta(h)$-relationship [e.g., *Poulovassilis*, 1962; *Mualem*, 1973, 1974; *Parlange*, 1976; *Kool and Parker*, 1987; *Hogarth et al.*, 1988; *Jaynes*, 1992; *Braddock et al.*, 2001; *Haverkamp et al.*, 2002b].

[9] Under field conditions, hysteresis is usually ignored because its influence is often masked by heterogeneities and spatial variability. However, many authors [e.g., *Nielsen et al.*, 1986; *Parker and Lenhard*, 1987; *Russo et al.*, 1989; *Heinen and Raats*, 1997; *Otten et al.*, 1997; *Whitmore and Heinen*, 1999; *Si and Kachanoski*, 2000; *Brutsaert*, 2005] have shown it to be important in simulations of water transfer, solute transport, multiphase flow and/or microbial activities, and to disregard it leads to significant errors in predicted fluid distributions with concomitant effects on solute transport and contaminant concentrations [e.g., *Gilham et al.*, 1976; *Hoa et al.*, 1977; *Kool and Parker*, 1987; *Kaluarachchi and Parker*, 1987; *Mitchel and Mayer*, 1998].

[10] Besides its effect on the flow behavior of water transfer, another aspect of hysteresis is nearly completely overlooked in the literature. Neglecting hysteresis and, hence, the history of drying and wetting cycles prior to measurement of the water retention data points, may well introduce an uncertainty in the choice of the appropriate equation to be used for the parameter identification. When equation (1) is chosen to represent the main loop of hysteresis, then all intermediate curves are described either by equations different from equation (1) or by equation (1) but with different system parameters. This is, what ever the hysteresis model used. As field measurements generally do not belong to the main loop, the use of equation (1) may often lead to a wrong interpretation of field measurements for the estimation of water retention system parameters with unreliable parameter values. In practice, users are rarely aware of this difficulty since generally only one set of drying data is measured making comparison impossible. Such erratic interpretation of water retention field data in the literature will probably be far more common than expected. As soil system parameters are generally compiled in soil databases for establishing statistical correlations of the type of pedotransfer functions [e.g., *Rawls and Brakensiek*, 1985; *Vereecken*, 1992; *Schaap and Leij*, 1998; *Schaap et al.*, 1998], one easily understands the difficulties that may cause the wrong interpretation of field data.

[11] The objective of this paper is to illustrate potential pitfalls with the estimation and use of retention parameters for field studies when hysteresis is neglected. The results will be illustrated with three examples, two taken from the literature and one from a recent field experiment. The purpose is not to validate the particular hysteresis model used for this study (as that is already presented elsewhere), but rather to draw the reader's attention to the fact that soil system parameters often presented in the literature to four significant figures, should be considered with precaution. Especially when only one set of data is measured without the possibility of comparison, the lack of information on the history of drying and wetting prior to the measurements is an important source of errors. Some guidelines to avoid possible pitfalls are addressed.

## 2. Theoretical Aspects

[12] A schematic representation of hysteresis for the soil water retention curve is shown in Figure 1. The boundary hysteresis loop consists of the main wetting curve (MWC) and main drying curve (MDC). If the wetting process is truncated and reversed to drying at a pressure head $h_{st1d}$ on the main wetting curve, a primary drying curve (PDC) results. Similarly, a primary wetting curve (PWC) departs from the main drying curve at a pressure head $h_{st1w}$ on the main drying curve and finishes at saturation $\theta_S$ (Figure 1). In general, any wetting (or drying) curve is defined by its point of departure from and arrival at a drying (or wetting) curve of a scanning order one lower (i.e., closed loops). For example, in Figure 1, a secondary drying curve (SDC) departs from the primary wetting curve (PWC) at some pressure head $h_{st2d}$ and rejoins the primary wetting curve at the point ($\theta_{st1w}$, $h_{st1w}$) where the PWC departed from its drying parent (MDC). Further drying continues then along the MDC.

[13] Theoretically, it should be possible to describe this hysteretic behavior from first principles [e.g., *Hassanizadeh and Gray*, 1993]. However, the problem remains largely unsolved, and our rather sketchy understanding of soil structure suggests that only a few soil models will yield to this approach. Instead, the description of hysteresis in soils remains often based on *Poulovassilis'* [1962] application of the independent domain theory with a more or less complicated interpolation technique to estimate the scanning curves from both main drying and wetting curves [e.g.,
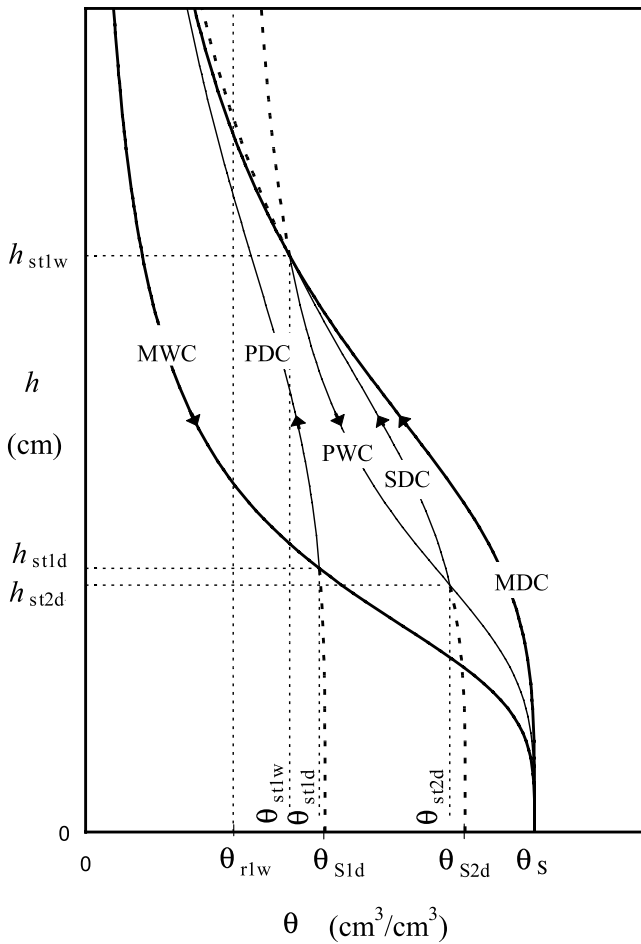
**Figure 1.** Schematic diagram of the hysteresis model with the main wetting curve (MWC), the main drying curve (MDC), a primary wetting curve (PWC) departing from the MDC at the point ($\theta_{st1w}$, $h_{st1w}$), a primary drying curve (PDC) departing from the MWC at the point ($\theta_{st1d}$, $h_{st1d}$), and a secondary drying curve (SDC) starting from the PWC at the point ($\theta_{st2d}$, $h_{st2d}$).

*Topp*, 1971; *Mualem*, 1974; *Mualem and Miller*, 1979; *Scott et al.*, 1983; *Kool and Parker*, 1987; *Parker and Lenhard*, 1987].

[14] An alternative approach has been presented by *Parlange* [1976] and was based on the concept of rational extrapolation. This theory requires only one boundary curve of the hysteresis envelope to predict the other boundary curve plus all the scanning curves in between. Even though the concept is very robust [e.g., *Hogarth et al.*, 1988; *Viaene et al.*, 1994; *Liu et al.*, 1995], it had the inconvenience of imposing a main wetting curve (MWC) without an inflection point and was therefore a priori only appropriate to use in combination with the *Brooks and Corey* [1964] water retention equation [*Haverkamp and Parlange*, 1986; *Hogarth et al.*, 1988]. *Si and Kachanoski* [2000] did not limit themselves to a Brooks and Corey relationship in their application of the *Parlange* [1976] hysteresis model. Like *Viaene et al.* [1994], *Si and Kachanoski* [2000] concluded that the model of Parlange was the best one when only one main scanning curve is used. In a later study, *Braddock et*

*al.* [2001] developed a pair of recurrence relations able to provide numerically relationships between wetting and drying phases to any order. It was only recently, that the rational extrapolation concept was reformulated analytically for the van Genuchten water retention equation using simple geometric scaling conditions [*Haverkamp et al.*, 2002b]. This latter model is considered here.

## 3. Model Description

[15] The ensemble of hysteresis curves are grouped into two families: the wetting and the drying family. The curves belonging to the same family are classified as a function of their scanning order; that is, starting at the main curve the series of scanning curves ascend the rank of scanning orders following the sequence of primary, secondary and tertiary scanning curves up to the scanning cycle of the order $k$. Obviously, when $k = 0$ we refer to the main curve.

[16] Starting with the wetting family, all curves, whatever their scanning order, have the form of the normalized van Genuchten water retention equation (1):

$$\theta_w^* \equiv \frac{\theta - \theta_{rkw}}{\theta_{Skw} - \theta_{rkw}} = \left[1 + \left(\frac{h}{h_{gkw}}\right)^{n_{kw}}\right]^{-m_{kw}}, \qquad (3)$$

where the subscript "w" refers to the wetting family, and "$k$" to the scanning order. Similarly, all curves of the drying family are given by:

$$\theta_d^* \equiv \frac{\theta - \theta_{rkd}}{\theta_{Skd} - \theta_{rkd}} = \left[1 + \left(\frac{h}{h_{gkd}}\right)^{n_{kd}}\right]^{-m_{kd}}, \qquad (4)$$

where the subscript "d" refers to the drying family. The shape parameters $m_{kw}$, $n_{kw}$ and $m_{kd}$, $n_{kd}$ are supposed to be related through equation (2).

[17] The definitions of equations (3) and (4) imply that all curves whatever their family and scanning order, have shape similarity, which does not necessarily mean shape identity. Each curve is characterized, a priori, by its specific shape parameters ($m_{kw}$ or $m_{kd}$), pressure head scale parameter ($h_{gkw}$ or $h_{gkd}$) and water content scale parameters $\theta_{Skw}$ and $\theta_{rkw}$, or $\theta_{Skd}$ and $\theta_{rkd}$ depending upon the starting and end points of the curves. For example, the PDC (Figure 1) which departs from the MWC at a point ($\theta_{st1d}$, $h_{st1d}$) ends at $\theta_{r1d} = 0$, and can be prolonged beyond the hysteresis envelope to the $\theta$-axis (dashed line). When $h = 0$ then $\theta = \theta_{S1d}$, which is fully determined by the starting point $\theta_{st1d}$ at which the primary drying curve departs. Although the physical meaning of the water content scaling parameter $\theta_{S1d}$ is slightly abstract, its value is mathematically well defined. The residual water content values of the various scanning curves are mathematically defined in a similar way, i.e., when $h \to -\infty$ then $\theta \to \theta_r$. For example, for the PWC (Figure 1) $\theta_r = \theta_{r1w}$, even though its value lies outside the hysteresis envelope. The loop for the main wetting (MWC) and drying (MDC) curve should obviously be closed with $\theta_{S0w} = \theta_{S0d} = \theta_S$ and $\theta_{r0w} = \theta_{r0d} = 0$. This condition implies that changes in the volume of entrapped air during rewetting owing to temperature differences [*Hopmans and Dane*, 1986] are disregarded. The concept of nonclosed hysteresis loops such as used by *Basile et al.* [2003] in trying to
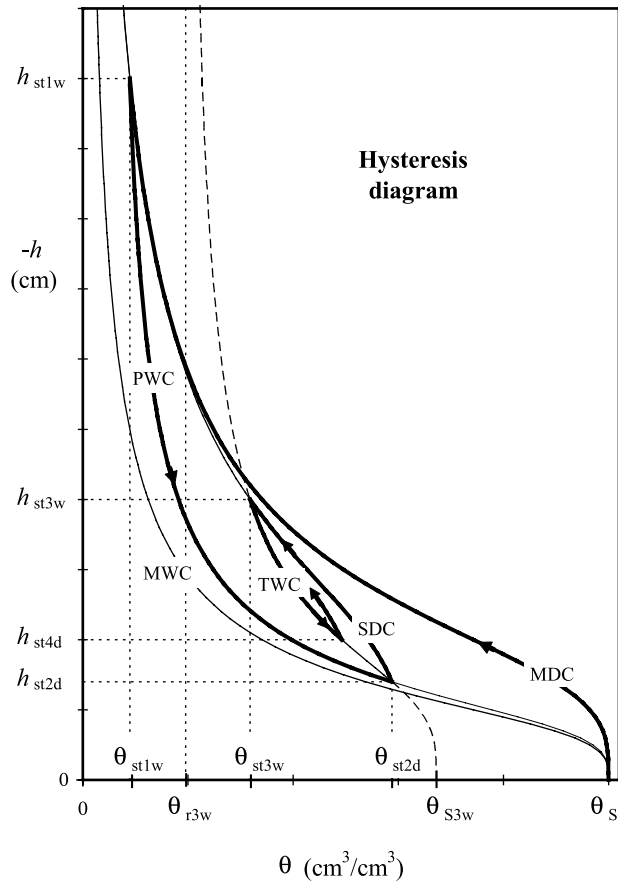
**Figure 2.** Schematic diagram of the hysteresis model showing a hypothetical wetting and drying path starting at $\theta_S$ the soil dries following the main drying curve (MDC); reversing to wetting at the point ($\theta_{st1w}$, $h_{st1w}$) the soil wets following the primary wetting curve (PWC); reversing again to drying at the point ($\theta_{st2d}$, $h_{st2d}$) the soil dries following the secondary drying (SDC); and reversing again to wetting at the point ($\theta_{st3w}$, $h_{st3w}$) the soil wets following the tertiary wetting curve (TWC).

explain the differences between field and laboratory data, are not considered for this study. These differences are probably strongly dependent on changes in soil structure and incompatibilities between representative volumes, rather than on hysteresis effects when changing from field to laboratory soils. Our study only considers soils whose structural properties do not change, and have a maximum soil water content which is different from the soil porosity owing to air entrapment.

[18] In their extensive study, *Haverkamp et al.* [2002b] derived three geometrical scaling conditions for the system parameters of equations (3) and (4) described above.

[19] 1. The first condition concerns the shape parameters. All curves of both wetting and drying families, independent of their scanning order, have identical shape parameters:

$$
\left.
\begin{aligned}
m &= m_{mw} = m_{1w} = m_{2w} = \ldots\ldots = m_{kw} = m_{kd} = \ldots\ldots m_{2d} = m_{1d} = m_{md} \\
n &= n_{mw} = n_{1w} = n_{2w} = \ldots\ldots = n_{kw} = n_{kd} = \ldots\ldots n_{2d} = n_{1d} = n_{md}
\end{aligned}
\right\}.
$$
(5)

This result is perfectly consistent with the concept of a soil specific shape index [*Haverkamp et al.*, 2005; *Leij et al.*, 2005] and was earlier used by various empirically based hysteresis models presented in the literature [e.g., *Scott et al.*, 1983; *Kool and Parker*, 1987; *Parker and Lenhard*, 1987]. As a consequence of equation (5), the shape parameters will be denoted hereafter as $m$ and $n$ only without any particular subscript.

[20] 2. The second condition defines the relation between the pressure head scale and the water content scale specific to each curve in wetting or drying. For the main wetting and drying curves (MWC and MDC), the relation between $h_{g0d}$ and $h_{g0w}$ is given by

$$
h_{g0d} = \alpha\, h_{g0w},
$$
(6)

where $\alpha$ is a parameter dependent on $m$ and $n$ only:

$$
\left.
\begin{aligned}
\alpha &= [1 + mn]^{1/mn} && \text{for} && 0 < mn \le 1 \\
\alpha &= 2 && \text{for} && mn > 1
\end{aligned}
\right\}.
$$
(7)

The equations (6) and (7) define the link between the pressure scale parameters of curves of the same loop but different families (i.e., main wetting curve $\Longleftrightarrow$ main drying curve). The link between the parameters of curves belonging to the same family but different scanning order (i.e., main wetting curve $\Longleftrightarrow$ $k$th-order scanning wetting curve) is given by

$$
\frac{h_{gkw}}{h_{g0w}} = \left[\frac{\theta_S}{\theta_{Skw} - \theta_{rkw}}\right]^{1/mn}
$$
(8)

and

$$
\frac{h_{gkd}}{h_{g0d}} = \left[\frac{\theta_S}{\theta_{Skd} - \theta_{rkd}}\right]^{1/mn}.
$$
(9)

[21] 3. Finally, the third condition determines the water content scale parameters. They are specific to the family and the scanning order of each particular curve (i.e., the hysteresis history) and are calculated according to their points of departure and arrival. The equations are based on geometrical scaling as shown schematically in Figure 1 and are directly derived from equations (3) and (4). Each scanning curve rejoins the point of departure of its parent curve; hence, the constraints such as the need for scanning curves to be closed and to lie inside curves of a lower order are automatically satisfied. It leads to the following specific conditions $\theta_{S1w} = \theta_{S0w} = \theta_{S0d} = \theta_S$ and $\theta_{r1d} = \theta_{r0d} = \theta_{r0w} = 0$.

[22] Given the saturated water content, the model allows for the prediction of all main, primary and higher-order scanning curves from knowledge of only one curve. The functioning of the hysteresis model is illustrated by Figure 2. It shows the prediction of the $h(\theta)$ relations for the hypothetical case of alternating wetting and drying passing through the reversal pressure heads $h_{st1w}$, $h_{st2d}$, $h_{st3w}$ and $h_{st4d}$ following scanning curves of increasing order. Beyond the third- or fourth-order scanning curves the hysteretic effect usually becomes small (Figure 2).

Complete and detailed information on the cascade calculations of the main and scanning curve parameters, is presented in the work of *Haverkamp et al.* [2002b] and *Ferraris* [2007].

[23] The model description given above clearly shows that the choice of the correct water retention equation (depending on the wetting/drying history) is crucial for an appropriate interpretation of field measurements. Since in practice measurements do not belong to the main loop, the use of equation (1) will necessarily lead to erroneous parameters estimation.

## 4. Material and Methods

[24] Two types of soil water retention data have been used for the analysis of hysteresis effects on soil characterization: (1) literature data taken from *Dane and Hruska* [1983] and *Haverkamp et al.* [1997]; and (2) field data collected at the experimental station (900 m²) of the Agricultural Faculty of the Università degli Studi di Torino at Grugliasco/ Italy [*Ferraris*, 2007]. Following *Natural Resources Conservation Service* (*NRCS*) [1960], the three soils belong to two different texture classes, i.e., "sand" and "silt loam."

[25] Starting with the literature data, the sand soil 1310 of the UNSODA soil database [*Leij et al.*, 1996] is considered first. The original water retention data were determined by *Dane and Hruska* [1983] who carried out a laboratory experiment using the internal drainage method [e.g., *Hillel*, 1980; *Libardi et al.*, 1980; *Vachaud et al.*, 1981] on an air-dried soil column with a dry bulk density ($\rho_d$) of 1.60 g/cm³. The experiment was started by wetting the soil column to give the wetting data. After saturation of the surface layer was achieved, infiltration was stopped and the drying process was measured.

[26] The second soil chosen from literature is the silt loam from the plain of La Mancha in Spain, on which *Haverkamp et al.* [1997] carried out a field experiment to determine its soil hydraulic characteristics by using the internal drainage method as well. The in situ experiment was started by wetting a naturally dried soil (no rain for more than 5 months with air temperatures around 50°C at midday) with a large 2-m-diameter ring infiltrometer to provide the wetting data. After 6 days, the infiltration was stopped and the drying process was measured. A dry bulk density ($\rho_d$) of 1.23 g/cm³ was observed.

[27] To analyze both sets of literature data, two scenarios are considered. The first scenario examines individually the data set of drying and of wetting without taking into account the possible existence of hysteresis. To do so, the water retention system parameters of each data set are estimated by fitting the van Genuchten model (equation (1)) to the measured $h(\theta)$ data using the Gauss-Marquardt method [*van Genuchten et al.*, 1991]. The goodness of fit is expressed by:

$$s(e) = \sqrt{\frac{\sum_{i=1}^{N_p} [\theta(h_i) - \theta_i]^2}{N_p - 1}}, \quad (10)$$

where $e$ is a variable associated with the equation error which is supposed to follow a normal distribution (centered at zero) with a finite variance $\sigma^2(e)$; $s(e)$ is the estimator of the standard deviation $\sigma(e)$; the subscript "$i$" refers to the sample measurements ($\theta_i$, $h_i$) with $i = 1, \ldots, N_p$; and the water content values $\theta(h_i)$ are calculated by equation (1). The user index $k_m$ is constrained at $k_m = 2$ reducing the number of unknown shape parameters to one. However, the constraint on the water content scale parameter $\theta_r$ is not imposed. Both cases with $\theta_r = 0$ and $\theta_r \neq 0$ are considered.

[28] The second scenario examines the drying and wetting data sets simultaneously in the framework of the hysteresis model described above. As both infiltration experiments have started with an air-dried soil column, the wetting data can be attributed to a primary wetting curve (PWC) expressed by equation (3) with $k = 1$ and $\theta_{S1w} = \theta_S$:

$$\frac{\theta - \theta_{r1w}}{\theta_S - \theta_{r1w}} = \left[1 + \left(\frac{h}{h_{g1w}}\right)^n\right]^{-m}. \quad (11)$$

Fitting this equation to the measured wetting data and minimizing condition [10], allows for the identification of the four unknown system parameters: $\theta_S$, $\theta_{r1w}$, $h_{g1w}$ and $m$. Then the secondary drying curve (SDC) is predicted with these wetting parameters, and compared to the measured drying data. To do so, the SDC given by equation (4) with $k = 2$ is expressed as a function of the wetting system parameters by a transformation of equations (4), (6), (8) and (9):

$$\frac{\theta - \theta_{r2d}}{\theta_{S2d} - \theta_{r2d}} = \left[1 + \left(\frac{1}{\alpha}\right)^n \left(\frac{\theta_{S2d} - \theta_{r2d}}{\theta_S - \theta_{r1w}}\right)^{1/m} \left(\frac{h}{h_{g1w}}\right)^n\right]^{-m}. \quad (12)$$

This equation still involves two unknowns: $\theta_{S2d}$ and $\theta_{r2d}$. Because the SDC departs from the PWC at the starting point ($\theta_{st2d}$, $h_{st2d}$), the combination of equations (11) and (12) allows to determine each SDC as a function of its starting water content value $\theta_{st2d}$ following the identification procedure given by *Haverkamp et al.* [2002b].

[29] As will be shown in the section 5, the above literature data provides strong evidence that the interpretation of water retention data can be quite delicate for parameter identification if only one set of data is considered (e.g., either wetting or drying) without taking into account the wetting and/or drying history prior to measurements. Introduction of the hysteresis concept helps to explain the discrepancies in data interpretation and to conceptualize the measurements in a consistent way. However, the literature studies cited do not provide independent benchmark data to verify the correctness of the approach. For that reason, a field study was carried out at the experimental station of the University of Turin at Grugliasco/Italy. A detailed description of the experiment and its results are given by *Ferraris* [2007].

[30] A grass-covered field plot of roughly 1.3 ha was equipped with an automatic data acquisition system of 80 tensiometers and 160 TDR probes installed at different depths down to $z = 200$ cm. Following *NRCS* [1960], the soil is defined as a sand with a clear A horizon over $0 < z <$

50 cm and a C horizon over $100 < z < 300$ cm. Between these two layers, a transition layer AC exists. A dry bulk density ($\rho_d$) of 1.5 g/cm$^3$ was observed for layer A, and 1.7 g/cm$^3$ for layer C [*Ferraris*, 2007].

[31] The experiment was planned following three stages. The first concerned an internal drainage test carried out under well-controlled initial conditions. This experiment was focused on the determination of the main drying characteristic parameters to be used as benchmark values for the following steps. At a second stage, the soil characteristic system parameters were determined under arbitrary field conditions using an inverse solution technique. These parameters obviously belong to some intermediate scanning curve either in wetting or drying. The last stage, and probably the most challenging, was aimed at the determination of the MDC parameters from those of the scanning curve by tracing back the history of the different scanning cycles all the way down to the main loop. Comparison of these parameters with the results obtained for stage 1 then allows to decide upon the correctness of the approach.

[32] A square of size 2 m × 2 m was selected within the field plot for the infiltration experiment which was carried out to determine the water retention characteristics by the internal drainage method. Being primarily interested in the A horizon ($0 < z < 50$ cm), the soil water content and pressure head were measured at two locations and three depths ($z = 30$, 45 and 60 cm). The experiment was performed during summer resulting in very dry initial soil water conditions. Great care was taken to saturate the A soil horizon in order to ensure the subsequent drying process would follow the main drying curve. After the wetting process was stopped, the surface was covered by a plastic sheet and drying was observed for a period of 52 days. The water retention data measured this way were considered to be the reference drying data belonging to the main drying curve (MDC).

[33] During the next spring, a second experiment was carried out to identify the soil characteristic parameters by using an inverse solution technique on the basis of field observations of rainfall intensities and soil water contents through time. This technique looks to obtain the best model output with a set of system parameters that are not necessarily the best description of the local field properties at a given depth but that, when introduced into the model, produce the best prediction of directly measurable quantities, such as the rate of infiltration and the rate of change of the soil water in the A horizon.

[34] Field observation showed that there was a rain period of 11 days with low-intensity rains (around 4 mm/hour). As a result, a quasi uniform initial water content profile was installed in the A horizon and no water ponding or surface runoff was observed. The period of simulation used for the parameter identification was chosen immediately after this rainfall period and lasted for 24 hours, i.e., Julian day 93.5 to 94.5.

[35] To make the inverse solution technique successful, at least two conditions should be satisfied: (1) the model used for the inverse procedure should be physically based and capable of describing the process with great precision; and (2) the model parameters should be independent of each other. For the numerical model, we have chosen the ADHYDRA code which solves *Richards'* [1931] equation using a mass conservative finite volume method [*Manzini and Ferraris*, 2004; *Ferraris*, 2007]. As to the system parameters, the four scale parameters have been chosen, i.e., the two water content scale parameters ($\theta_S$ and $\theta_r$), the pressure head ($h_g$) and the hydraulic conductivity at natural saturation ($K_S$). The shape parameters $m$ and $n$ were determined indirectly using the prediction technique on the basis of textural particle-size information [*Haverkamp et al.*, 2006].

[36] In order to take into account the history of wetting and drying prior to the experiment, the scale parameters have to be associated to a particular scanning curve. Following *Haverkamp et al.* [2002b] most of the hysteresis cycles are initially originated from the main drying curve (MDC). Consequently, the wetting scanning curves belong to cycles with odd scanning orders, i.e., $k = 1$, 3 or even 5. Since the soil profile was not saturated prior to the observation period (no runoff or ponding), the wetting scanning curve we are aiming for, was most likely departed from a secondary drying curve (SDC) rather than the main drying curve (MDC). Hence, the wetting cycle of the experiment followed a tertiary wetting curve (TWC) with the three water retention system parameters $\theta_{S3w}$, $\theta_{r3w}$ and $h_{g3w}$ to be determined by the inverse solution technique. A schematic representation of the water retention hysteresis cycle for this particular case is given in Figure 2.

[37] The objective function used to optimize the model's performance was to match the measured outgoing fluxes at the bottom of the A horizon which were calculated from the changes in spatial soil water content measured through an ensemble of 27 TDR probes. As an example, Figure 3 shows the time evolution of the cumulated fluxes measured at 50 cm depth. During the experiment, the outgoing evaporation flux at the soil surface was considered as negligible. The optimization algorithm was based on the grid search technique of *Duan et al.* [1992] and adapted to the parameter space of $\theta_{S3w}$, $\theta_{r3w}$, $h_{g3w}$ and $K_S$ following the scheme of *Ferraris and Carabelli* [1994].

[38] Once the four water retention scale parameters being determined, the complete series of hysteretic cycles have to be calculated backward, all the way down to the main loop in order to determine the benchmark system parameters $\theta_S$ and $h_{g0d}$ of the main drying curve. This implies to follow the path back from that illustrated in Figure 2: TWC → SDC → PWC → MDC. Using the hysteresis framework given by equations (3) and (4), such procedure involves 16 a priori unknown system parameters, i.e., $\theta_{S3w}$, $\theta_{r3w}$, $h_{g3w}$, $\theta_{st3w}$ and $h_{st3w}$ (TWC); $\theta_{S2d}$, $\theta_{r2d}$, $h_{g2d}$, $\theta_{st2d}$ and $h_{st2d}$ (SDC); $\theta_S$, $\theta_{r1w}$, $h_{g1w}$, $\theta_{st1w}$ and $h_{st1w}$ (PWC); and $\theta_S$ and $h_{gmd}$ of the MDC. However, the inverse solution technique provides three parameters $\theta_{S3w}$, $\theta_{r3w}$ and $h_{g3w}$, whereas the initial conditions determines the two values of $\theta_{st3w}$ and $h_{st3w}$ which leaves 11 unknown parameters to solve. The solution of this problem is not trivial but can be solved in cascade by combining equations (3), (4), (6), (8) and (9) following the same procedure as that used for the formulation of equations (11) and (12). A full detailed description of the algorithm is given by *Ferraris* [2007]. The main drying water retention system parameters calculated in this way are then compared with the values of $\theta_S$
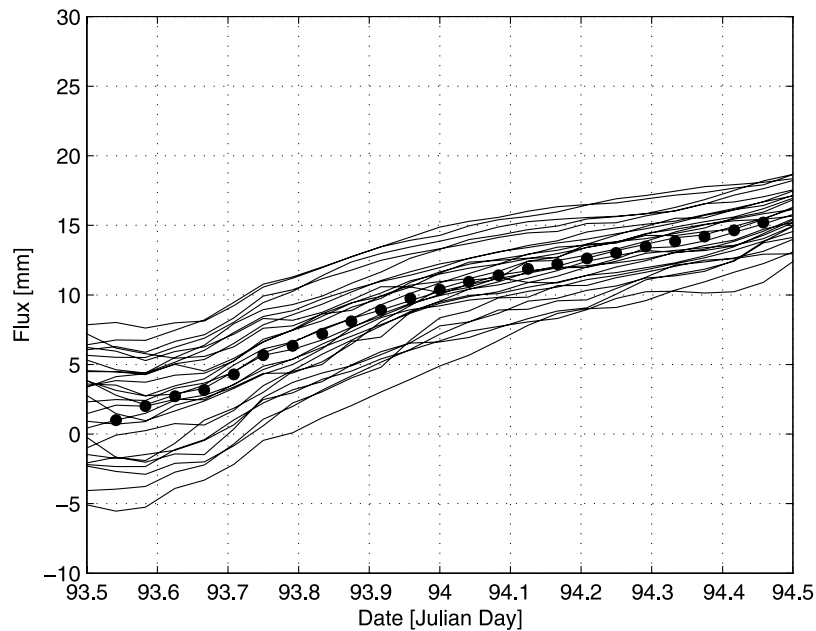
**Figure 3.** Time evolution of cumulated outgoing fluxes measured at depth $z = 50$ cm through an ensemble of 27 TDR probes (solid lines) and calculated by numerical solution using best fit system parameters (solid circles).

and $h_{g0d}$ determined by using the internal drainage method described before.

## 5. Results and Analysis

[39] The drying and wetting water retention data measured for the sand soil 1310 are presented in Figures 4a and 4b. The measurement errors associated with water content and soil water pressure head are taken equal to $\sigma(\theta) = \pm 0.01$ cm$^3$/cm$^3$ and $\sigma(h) = \pm 2$ cm, respectively [*Sinclair and Williams*, 1979; *Haverkamp et al.*, 1984]. These values are generally accepted for laboratory experiments.

[40] For the case where the effect of hysteresis is disregarded, the data sets of drying and wetting are considered individually. Hence, this situation (corresponding to the first scenario explained above) would have occurred when taking water retention measurements without having the possibility of comparison with the other curve. The best fit procedure with equation (1) gives very different water retention curves (Figure 4a) with two sets of totally different system parameters (Tables 1a and 1b). This result which is independent of the constraint imposed on $\theta_r$, clearly shows the difficulty in reading correctly the water retention measurements. The variation is particularly important for the scale parameters $\theta_S$ and $h_g$. Taking the example of the water content scale parameter (Tables 1a and 1b), $\theta_S$ changes from 0.40 to 0.16 cm$^3$/cm$^3$ depending on whether the wetting or drying data are used for the parameter identification. For the same soil, such a result is obviously inconceivable. The water content value $\theta_S = 0.16$ cm$^3$/cm$^3$ becomes even more unrealistic when compared with the soil porosity $\varepsilon = 0.3962$ cm$^3$/cm$^3$ resulting in a ratio $\theta_S/\varepsilon = 0.41$. This ratio is considerably smaller than the interval $0.8 < \theta_S/\varepsilon < 1$ classically reported [*Rogowski*, 1971]. However, when only one curve is available there is a priori no reason to doubt about the value $\theta_S = 0.16$ cm$^3$/cm$^3$ as no comparison is available.

[41] The explanation for this discrepancy lies in the history of the experimental conditions. At the moment the infiltration was stopped, only the top section of the soil column was saturated whereas at a greater depth the soil was still not saturated. Hence, at these depths, the drying process departed from the wetting curve before saturation was achieved. When introducing the effects of hysteresis through the use of equations (11) and (12), the results become suddenly fully consistent (Figure 4b) with realistic system parameters. The good agreement between the SDC and the measured drying data (Figure 4b) is even more remarkable if one realizes that the SDC is not a fitted curve, but a predicted curve calculated with the system parameters obtained by identification on the wetting data.

[42] The second test case concerns the silt loam. The drying and wetting water retention data are presented in Figures 5a and 5b. While the wetting data are aligned along the wetting curve, the drying data are scattered as a function of soil depth. When considering the drying data only, these results seem to indicate a layered soil profile with a homogeneous top layer over the first 50 cm, followed by two layers at 70 and 90 cm depth. The measurement errors associated with water content and pressure head are slightly bigger than those chosen for the laboratory experiment, i.e., $\sigma(\theta) = \pm 0.02$ cm$^3$/cm$^3$, and $\sigma(h) = \pm 5$ cm.

[43] When estimating the system parameters of the water retention equation by fitting individually equation (1) (corresponding to scenario 1) to the measured $h(\theta)$ data (Tables 2a and 2b), the results are again very confusing as for the sand data discussed before. The scale parameters vary much more than the shape parameter (e.g., $h_g$ changes
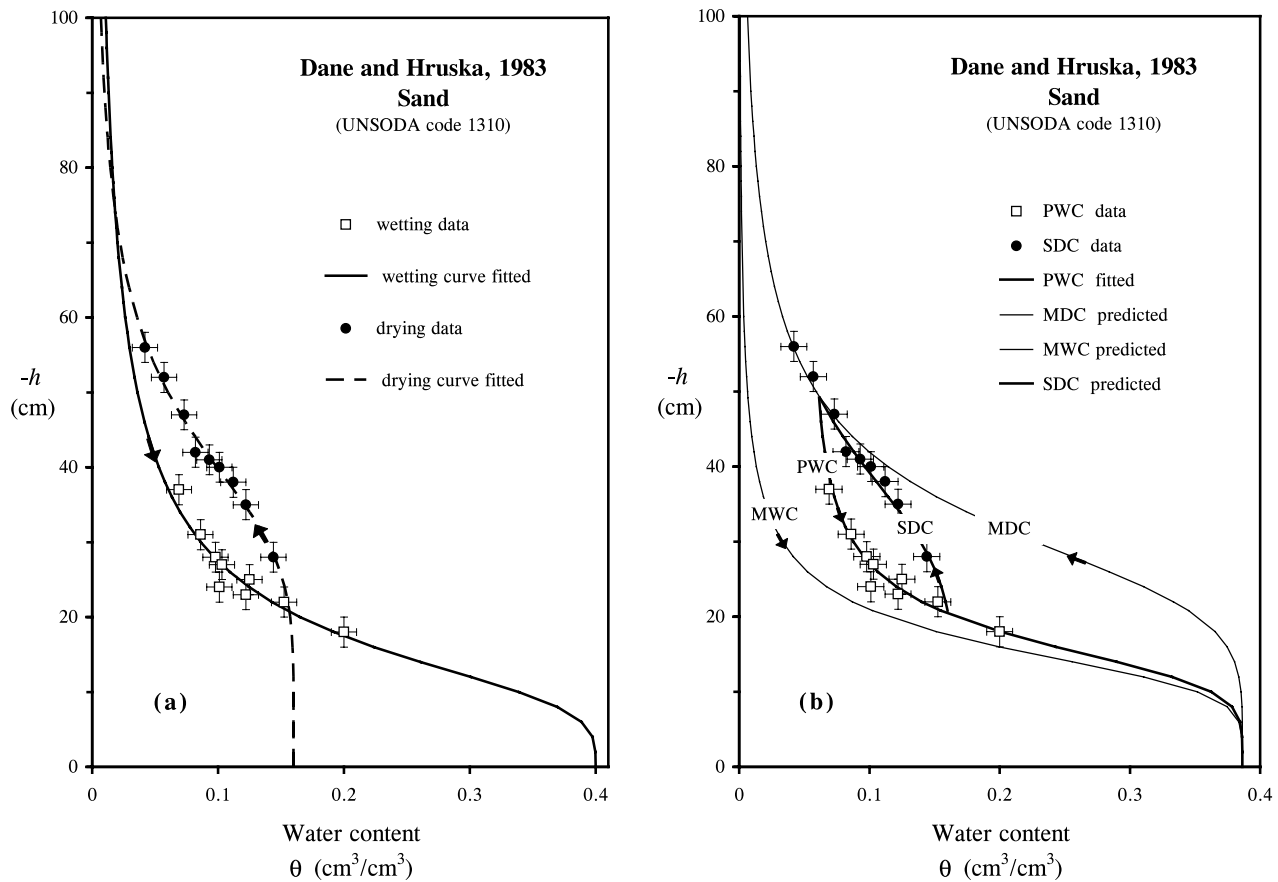
**Figure 4.** Water retention curves fitted to wetting (open squares) and drying (solid circles) data measured for the sand soil taken from *Dane and Hruska* [1983] using (a) the van Genuchten model (equation (1)) with the constraints $k_m = 2$ and $\theta_r = 0$ and neglecting hysteresis effects and the (b) primary wetting curve (PWC) fitted to the measured wetting data (open squares) together with the predicted secondary drying curve (SDC) and the experimental drying data (solid circles), including hysteresis. The horizontal and vertical bars correspond to the measurement errors in water content and soil water pressure head (i.e., $\sigma(\theta) = \pm 0.01$ cm³/cm³ and $\sigma(h) = \pm 2$ cm) associated with each observation ($\theta_i$, $h_i$). Parameter values for Figures 4a and 4b are given in Tables 1a and 1b.

from 391.0 to 827.8 cm). The ambiguity in interpretation of the measurements, is provoked once again by the lack of knowledge on the history of the experimental conditions. That is to say, when the infiltration was stopped after 6 days, the lower horizons (e.g., $z = 70$ and 90 cm) were not yet saturated; hence, the drying process measured at lower depths started from pressure head values much bigger (in absolute values) than those in the surface layer. So, the data

scatter that initially seemed to indicate the existence of a layered soil profile, is only due to a retardance in the wetting of the homogeneous soil profile. The latter conclusion is obviously very different from that assumed in the beginning.

[44] This result is backed up by the data analysis using the hysteresis concept expressed by equations (11) and (12). It homogenizes the ensemble of wetting and drying data of

**Table 1a.** Characteristic Soil Parameters Obtained by Fitting the Water Retention Model of van Genuchten to the Sand Soil of *Dane and Hruska* [1983] Disregarding Possible Hysteresis Effects[a]

| | Fitting with Equation (1), Wetting Curve | | | | | Fitting with Equation (1), Drying Curve | | | | |
|---|---|---|---|---|---|---|---|---|---|---|
| | $\theta_S$ (cm³/cm³) | $\theta_r$ (cm³/cm³) | $-h_g$ (cm) | $m$ | $s(e)$ (cm³/cm³) | $\theta_S$ (cm³/cm³) | $\theta_r$ (cm³/cm³) | $-h_g$ (cm) | $m$ | $s(e)$ (cm³/cm³) |
| Constraint | 0.400 | 0.0 | 12.55 | 0.465 | $1.1 \times 10^{-2}$ | 0.1600 | 0.0 | 38.94 | 0.625 | $3.8 \times 10^{-3}$ |
| Nonconstraint | 0.400 | 0.0531 | 14.47 | 0.611 | $9.2 \times 10^{-3}$ | 0.1493 | 0.0 | 41.46 | 0.661 | $4.4 \times 10^{-3}$ |

[a]The data correspond to disregarding hysteresis and fitting equation (1) separately to the wetting and drying data.

**Table 1b.** Characteristic Soil Parameters Obtained by Fitting the Water Retention Model of van Genuchten to the Sand Soil of *Dane and Hruska* [1983] Considering Hysteresis Effects[a]

| Fitting With Equation (11), Primary Wetting Curve | | | | | Prediction With Equation (12), Secondary Drying Curve | | | | |
|---|---|---|---|---|---|---|---|---|---|
| $\theta_S$ $(cm^3/cm^3)$ | $\theta_{r1w}$ $(cm^3/cm^3)$ | $-h_{g1w}$ $(cm)$ | $m$ | $s(e)$ $(cm^3/cm^3)$ | $\theta_{S2d}$ $(cm^3/cm^3)$ | $\theta_{r2d}$ $(cm^3/cm^3)$ | $-h_{g2d}$ $(cm)$ | $m$ | $s(e)$ $(cm^3/cm^3)$ |
| 0.3863 | 0.0545 | 14.81 | 0.618 | $9.8 \times 10^{-3}$ | 0.1644 | 0.0054 | 37.18 | 0.618 | $5.3 \times 10^{-3}$ |

[a]The data include hysteresis effects fitting the primary wetting curve (equation (11)) to the wetting data together with equation (12) to find the system parameters predicted for the secondary drying curve.

the entire soil profile in a fully consistent way without any soil layers (Figure 5b). The system parameters identified by fitting the PWC to the wetting data, allow the prediction of the three SDCs in very good agreement with the independently measured drying data. Note that the standard deviations $s(e)$ observed for the prediction are of the same order of magnitude as those calculated by the best fit procedure (Tables 2a and 2b).

[45] The foregoing results clearly demonstrate how the uncertainty in the choice of the appropriate water retention equation can lead to a completely wrong interpretation of field measurements when estimating the water retention system parameters. Moreover, if one realizes that the wetting curve is rarely measured under field conditions, the erratic interpretation of water retention field data will probably be far more common than expected.
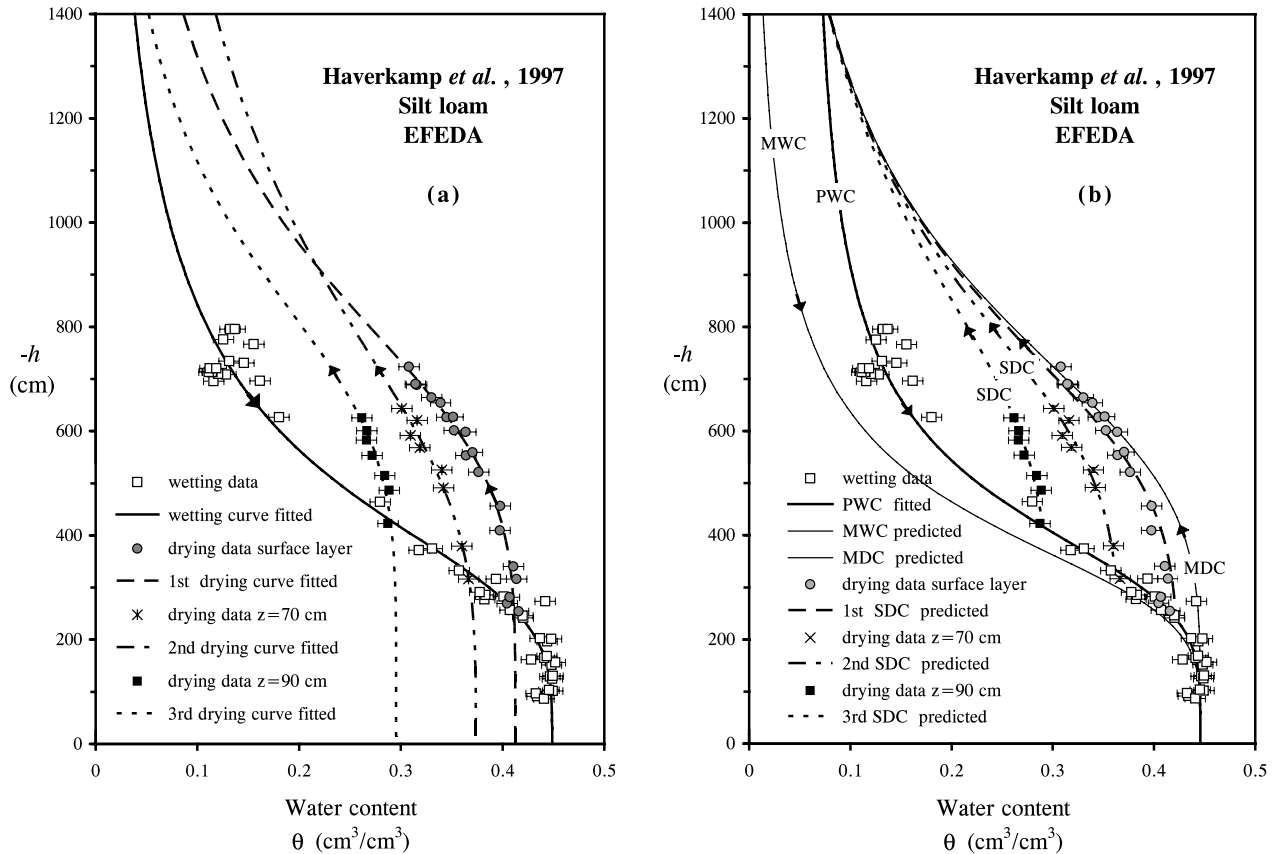


**Figure 5.** Water retention curves fitted to wetting (open squares) and drying (solid circles, crosses, and solid squares) data measured for the silt loam of *Haverkamp et al.* [1997] using (a) the van Genuchten model (1) with the constraints $k_m = 2$ and $\theta_r = 0$ and neglecting hysteresis effects and (b) the primary wetting curve (PWC) fitted to the measured wetting data (open squares) together with the various predicted secondary drying curves (SDC) and the experimental drying data (solid circles, crosses, and solid squares), including hysteresis. The horizontal and vertical bars correspond to the measurement errors in water content and soil water pressure head (i.e., $\sigma(\theta) = \pm 0.02$ cm$^3$/cm$^3$ and $\sigma(h) = \pm 5$ cm) associated with each observation $(\theta_i, h_i)$. Parameter values for Figures 5a and 5b are given in Tables 2a and 2b.

**Table 2a.** Characteristic Soil Parameters Obtained by Fitting the Water Retention Model of van Genuchten to the Silt Loam of *Haverkamp et al.* [1997] Disregarding Hysteresis

| Disregarding Possible Hysteresis Effects | Fitting With Equation (1), Wetting Curve | | | | | Fitting With Equation (1), Drying Curve[a] | | | | |
|---|---|---|---|---|---|---|---|---|---|---|
| | $\theta_S$ (cm$^3$/cm$^3$) | $\theta_r$ (cm$^3$/cm$^3$) | $-h_g$ (cm) | $m$ | $s(e)$ (cm$^3$/cm$^3$) | $\theta_S$ (cm$^3$/cm$^3$) | $\theta_r$ (cm$^3$/cm$^3$) | $-h_g$ (cm) | $m$ | $s(e)$ (cm$^3$/cm$^3$) |
| Constraint | 0.4487 | 0.0 | 391.01 | 0.490 | $1.6 \times 10^{-2}$ | 0.4125 | 0.0 | 779.86 | 0.566 | $4.6 \times 10^{-3}$ |
| Nonconstraint | 0.4457 | 0.0596 | 383.47 | 0.564 | $1.5 \times 10^{-2}$ | 0.4124 | 0.0269 | 765.30 | 0.574 | $4.5 \times 10^{-3}$ |
| Constraint | - | - | - | - | - | 0.3737 | 0.0 | 744.17 | 0.468 | $4.9 \times 10^{-3}$ |
| Nonconstraint | - | - | - | - | - | 0.3733 | 0.0218 | 732.60 | 0.479 | $4.9 \times 10^{-3}$ |
| Constraint | - | - | - | - | - | 0.2954 | 0.0 | 827.81 | 0.618 | $3.1 \times 10^{-3}$ |
| Nonconstraint | - | - | - | - | - | 0.2953 | 0.0213 | 813.40 | 0.621 | $3.1 \times 10^{-2}$ |

[a]Surface soil layer $0 < z < 50$ cm for the first two rows, soil layer $z = 70$ cm for the next two rows, and soil layer $z = 90$ cm for the last two rows.

[46] The last test case concerns the field experiment at Grugliasco. The first step of this experiment dealt with the application of the internal drainage method for the determination of the main drying data. As for the foregoing field experiment, the measurement errors associated with water content and water pressure head are respectively $\sigma(\theta) = \pm 0.02$ cm$^3$/cm$^3$ and $\sigma(h) = \pm 5$ cm. The estimation of the water retention system parameters by fitting the van Genuchten model equation (1) to the measured $h(\theta)$ data with the constraints $k_m = 2$ and $\theta_r = 0$ (Figure 6a), gives satisfying results with a standard deviation of $s(e) = 2.29$ $10^{-2}$ cm$^3$/cm$^3$ (Tables 3a and 3b). The fitted value of $\theta_S = 0.4326$ cm$^3$/cm$^3$ is big as compared to the total porosity $\varepsilon = 0.434$ cm$^3$/cm$^3$ estimated from the dry bulk density $\rho_d = 1.5$ g/cm$^3$. Even though this value is not impossible for structureless sand soils, it rather reflects the fact that the optimization of $\theta_S$ is an ill-posed problem. Variations in $\theta_S$ are compensated by those of $h_{g0d}$. This problem is illustrated by the surface plot of $s(e)$ which behaves as a quasi flat bottom valley (Figure 7).

[47] The second part of the Grugliasco experiment seeks to identify the water retention system parameters ($\theta_{S3w}$, $\theta_{r3w}$ and $h_{g3w}$) associated with the third wetting scanning curve by using an inverse solution technique on the basis of field observations of rainfall intensities and soil water content through time. To optimize the model's performance the objective function matched the outgoing fluxes at the bottom of the A horizon. As shown by Figure 3, the best model output gives good agreement with measured cumulative fluxes. The associated scale parameters are reported in Tables 3a and 3b.

[48] The tertiary wetting scanning parameters being determined, the last step of the Grugliasco experiment looks to trace back the hysteretic cycles down to the main drying curve in order to determine the benchmark system parameters $\theta_S$ and $h_{g0d}$. Theoretically the model allows for the prediction of all main, primary and higher-order scanning curves from the knowledge of only one curve such as the tertiary wetting curve, but still this task is not trivial as the equation system to be solved is complex. The results are shown in Figure 6b and Tables 3a and 3b. The predicted main drying curve shows very good agreement with the measured main drying data. The standard deviation $s(e) = 2.32$ $10^{-2}$ cm$^3$/cm$^3$ is nearly identical to that calculated for the internal drainage method $s(e) = 2.29$ $10^{-2}$ cm$^3$/cm$^3$ (Tables 3a and 3b). As to the system parameters $\theta_S$ and $h_{g0d}$, the predicted values are much the same as the bench mark values.

[49] The results of Figure 6b clearly show that the effect of hysteresis becomes less important for scanning cycles bigger than three. So, if the water retention data measured during the field campaign of stage 2 of the Grugliasco experiment would have been attributed to the fifth wetting scanning cycle rather than to the third as supposed in this study, then the prediction would still have been very similar to that presented in Figure 6b.

[50] The good agreement between the predicted and measured main drying results shows the correctness of the hysteresis model used in this study. At the same time, it confirms that the erratic interpretation of water retention field data shown in the three examples in this study is a realistic problem which unavoidably leads to large

**Table 2b.** Characteristic Soil Parameters Obtained by Fitting the Water Retention Model of van Genuchten to the Silt Loam of *Haverkamp et al.* [1997] Including Hysteresis

| Considering Hysteresis Effects | Fitting With Equation (11), Primary Wetting Curve | | | | | Prediction With Equation (12), Secondary Drying Curve[a] | | | | |
|---|---|---|---|---|---|---|---|---|---|---|
| | $\theta_S$ (cm$^3$/cm$^3$) | $\theta_{r1w}$ (cm$^3$/cm$^3$) | $-h_{g1w}$ (cm) | $m$ | $s(e)$ (cm$^3$/cm$^3$) | $\theta_{S2d}$ (cm$^3$/cm$^3$) | $\theta_{r2d}$ (cm$^3$/cm$^3$) | $-h_{g2d}$ (cm) | $m$ | $s(e)$ (cm$^3$/cm$^3$) |
| | 0.4457 | 0.0594 | 380.98 | 0.56 | $1.5 \times 10^{-2}$ | 0.4227 | 0.0002 | 735.71 | 0.561 | $9.8 \times 10^{-3}$ |
| | - | - | - | - | - | 0.3657 | 0.0007 | 779.06 | 0.561 | $5.4 \times 10^{-3}$ |
| | - | - | - | - | - | 0.2963 | 0.001 | 847.17 | 0.561 | $3.3 \times 10^{-3}$ |

[a]Surface soil layer $0 < z < 50$ cm for the first row, soil layer $z = 70$ cm for the second row, and soil layer $z = 90$ cm for the last row.
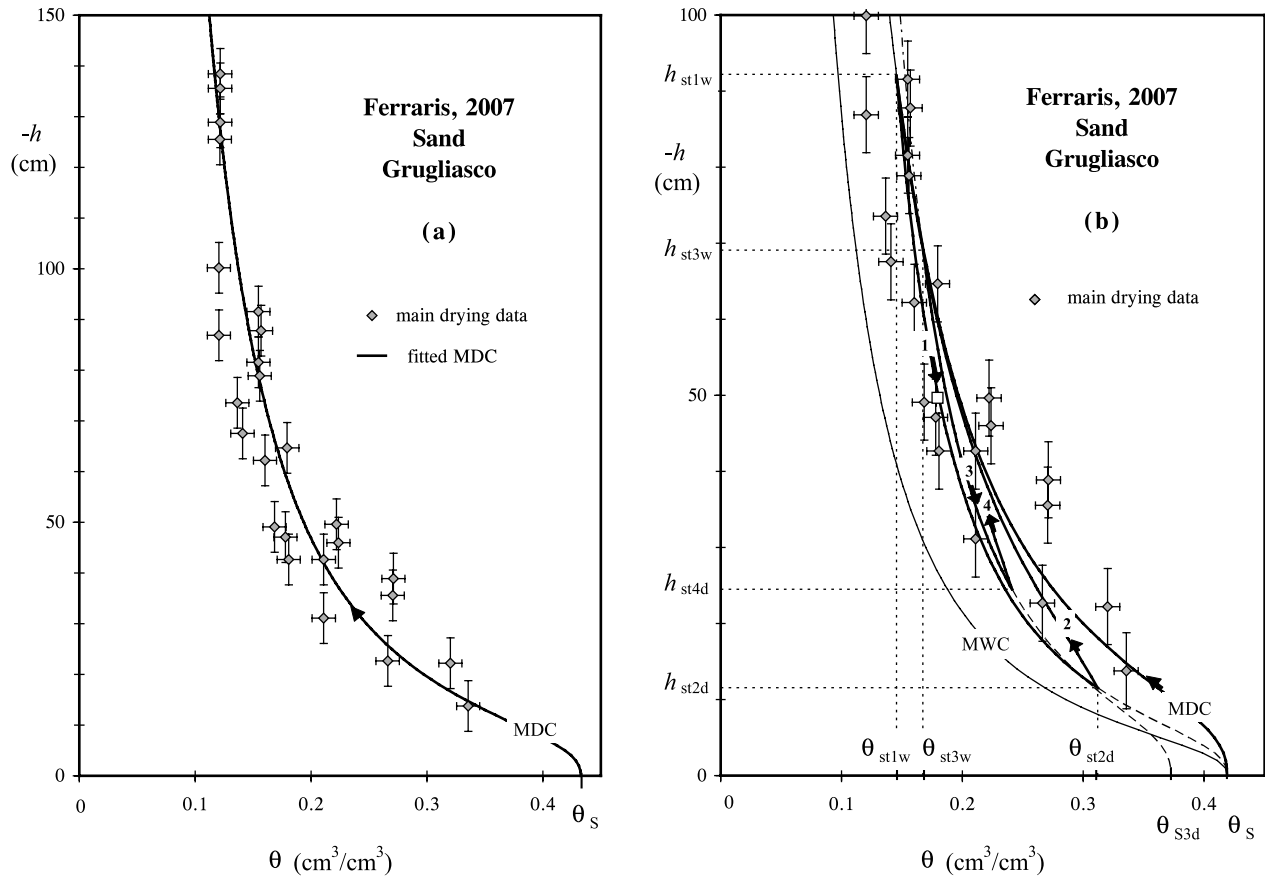
**Figure 6.** Water retention curves fitted to main drying data (solid diamonds) measured for the sand of Grugliasco [*Ferraris*, 2007] using (a) the van Genuchten model (1) with the constraints $k_m = 2$ and $\theta_r = 0$ and neglecting hysteresis effects and (b) predicted tertiary wetting (TWC), secondary drying (SDC), primary wetting (PWC), and main drying (MDC) curves and experimental main drying data (solid diamonds), including hysteresis. The horizontal and vertical bars correspond to the measurement errors in water content and soil water pressure head (i.e., $\sigma(\theta) = \pm 0.02$ cm$^3$/cm$^3$ and $\sigma(h) = \pm 5$ cm) associated with each observation ($\theta_i$, $h_i$). Parameter values for Figures 6a and 6b are given in Tables 3a and 3b.

uncertainties in the values of the water retention system parameters.

## 6.  Summary and Conclusions

[51] The objective of this paper is to illustrate potential pitfalls with the estimation and use of retention parameters for field studies when hysteresis is disregarded. In fact, neglecting hysteresis and, hence, the history of drying and wetting cycles prior to measurement of the water retention data points, introduces great uncertainty in the choice of the appropriate equation to be used for the parameter identification. This error often leads to a wrong interpretation of field measurements resulting into erratic values of the water retention system parameters. In practice, users are unfortunately rarely aware of this complication.

[52] This problem is put in evidence by the use of three examples representative for the test conditions under which soil characterization experiments are generally carried out. The first two test cases concerned literature data.

They clearly showed that the interpretation of water retention data belonging to wetting of drying scanning curves (such as is the case for most field experiments) systematically induces errors in the estimation of the water content and pressure head scale parameters ($\theta_S$ and $h_{g0d}$). Errors of more than 100% were observed. Only for main

**Table 3a.** Characteristic Soil Parameters Obtained by Fitting the Water Retention Model of van Genuchten to the Sand of Grugliasco Described by *Ferraris* [2007] Using the Internal Drainage Method[a]

| Type of Scanning Curve | Internal Drainage Method | | | | |
|---|---|---|---|---|---|
| | $\theta_S$ (cm$^3$/cm$^3$) | $\theta_{r0d}$ (cm$^3$/cm$^3$) | $-h_{g0d}$ (cm) | $m$ | $s(e)$ (cm$^3$/cm$^3$) |
| MDC | 0.4326 | 0.0 | 10.09 | 0.20 | 2.29 $10^{-2}$ |

[a]The data correspond to fitting equation (1) to the main drying data.

**Table 3b.** Characteristic Soil Parameters Obtained by Fitting the Water Retention Model of van Genuchten to the Sand of Grugliasco Described by *Ferraris* [2007] Using the Inverse Solution Technique[a]

| Type of Scanning Curve | Inverse Solution Technique | | | | | | | | |
|---|---|---|---|---|---|---|---|---|---|
| | $\theta_{Sk}$ $(cm^3/cm^3)$ | $\theta_{rk}$ $(cm^3/cm^3)$ | $-h_{gk}$ (cm) | $m$ | $s(e)$ $(cm^3/cm^3)$ | $\theta_{stkw}$ $(cm^3/cm^3)$ | $-h_{stkw}$ (cm) | $\theta_{stkd}$ $(cm^3/cm^3)$ | $-h_{stkd}$ (cm) |
| TWC | 0.3726[b] | 0.0554[b] | 8.62[b] | 0.20 | - | 0.1674[c] | 69.10[c] | - | - |
| SDC | 0.3302 | 0.0003 | 17.95 | 0.20 | - | - | - | 0.3118 | 11.55 |
| PWC | 0.4190 | 0.0484 | 6.32 | 0.20 | - | 0.1454 | 92.20 | - | - |
| MDC | 0.4190 | 0.0 | 11.13 | 0.20 | $2.32 \ 10^{-2}$ | - | - | - | - |

[a]Hysteresis effects are included by calculating the water retention system parameters of the hysteresis sequence TWC → SDC → PWC → MDC, starting from the best fit scale parameters $\theta_{S3w}$, $\theta_{r3w}$ and $h_{g3w}$ obtained by the inverse solution technique to find the prediction error of the MDC fitted to independently measured MDC data.
[b]Output values of the inverse solution technique.
[c]Measured initial conditions.

drying conditions, the uncertainty in the choice of the appropriate equation to be used for the parameter identification is avoided. The problem is particularly crucial when only one set of data is measured (which is generally the case), as the comparison with other data sets is not possible. Often, these difficulties are totally ignored.

[53] The third test case concerned a field experiment especially carried out for this study. It showed that the equational framework imposed by using the physically based hysteresis model, allows to trace back the history of scanning cycles prior to the measurements from the knowledge on only one scanning curve. It validated the correctness of the hysteresis model and thus confirmed that the errors found for the water content and pressure head sale parameters were not due to a bias in the model used for interpretation. The rigorous conditions of the hysteresis model reduced the uncertainties in the identifications of the water content and pressure head scale parameters ($\theta_S$ and $h_{g0d}$) from simple measurements.

[54] To avoid the potential pitfalls illustrated above, one should either operate under rigorously known experimental test conditions (e.g., main drying conditions) or include an hysteresis model into the data analysis. This latter point has already earlier been stressed by *Brutsaert* [2005], who wrote: "Certainly, the error resulting from taking into account a simplified hysteresis model will be much smaller than the unavoidably large errors resulting from uncertainties in the values of soil water flow parameters and from ignoring hysteresis altogether, as is currently still almost universal practice."
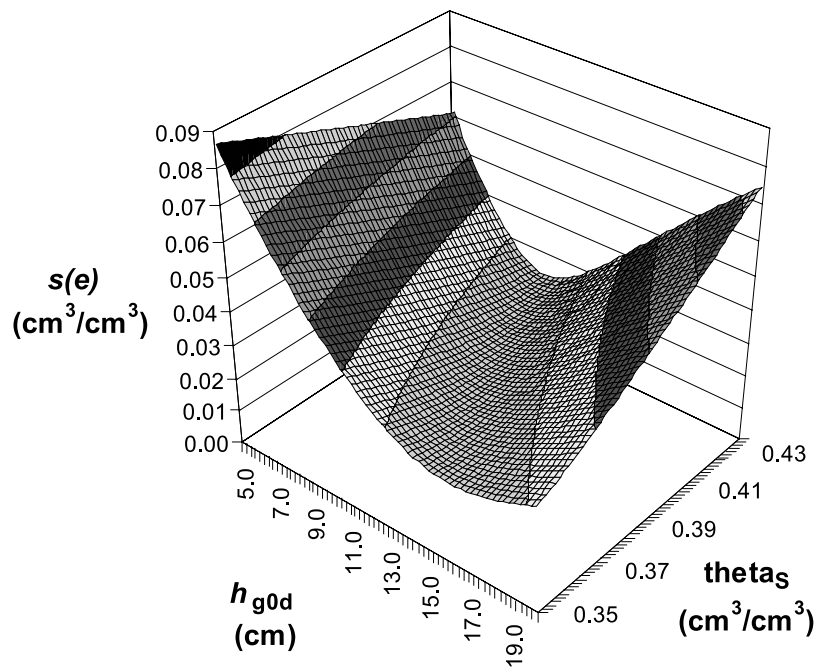


**Figure 7.** Standard deviation $s(e)$ as a function of both the water content ($\theta_S$) and pressure head ($h_{g0d}$) scale parameters.

# References

Assouline, S., D. Tessier, and A. Bruand (1998), A conceptual model of the soil water retention curve, *Water Resour. Res.*, 34, 223–231, doi:10.1029/97WR03039.

Basile, A., G. Ciollaro, and A. Coppola (2003), Hysteresis in soil water characteristics as a key to interpreting comparisons of laboratory and field measured hydraulic properties, *Water Resour. Res.*, 39(12), 1355, doi:10.1029/2003WR002432.

Braddock, R. D., J.-Y. Parlange, and H. Lee (2001), Application of a soil water hysteresis model to simple water retention curves, *Transp. Porous Media*, 44, 407–420, doi:10.1023/A:1010792008870.

Brooks, R. H., and A. T. Corey (1964), Hydraulic properties of porous media, *Hydrol. Pap. 3*, Colo. State Univ., Fort Collins, Colo.

Brutsaert, W. (1966), Probability laws for pore size distributions, *Soil Sci.*, 101, 85–92, doi:10.1097/00010694-196602000-00002.

Brutsaert, W. (2005), *Hydrology: An Introduction*, 605 pp., Cambridge Univ. Press, New York.

Burdine, N. T. (1953), Relative permeability calculations from pore-size distribution data, *Trans. Am. Inst. Min. Metall. Pet. Eng.*, 198, 71–78.

Dane, J. H., and S. Hruska (1983), In-situ determination of soil hydraulic properties during drainage, *Soil Sci. Soc. Am. J.*, 4, 619–624.

Duan, Q., S. Sorooshian, and V. Gupta (1992), Effective and efficient global optimization for conceptual rainfall-runoff models, *Water Resour. Res.*, 28, 1015–1031, doi:10.1029/91WR02985.

Ferraris, S. (2007), Méthode de caractérisation hydrodynamique du sol à l'échelle globale à partir des mesures météorologiques: Comparaison avec des mesures locales dans un sol sableux de Grugliasco avec prise en compte d'hystérésis, internal report, 195 pp., Dep. of Econ. and Agric., For., and Environ. Eng., Univ. of Turin, Turin, Italy.

Ferraris, S., and S. Carabelli (1994), Misura delle proprietà idrauliche dei substrati, *Colture Protette*, 2, 87–95.

Gardner, W. R. (1958), Some steady state solutions of the unsaturated moisture flow equation with application to evaporation from a water table, *Soil Sci.*, 85, 228–233.

Gilham, R. W., A. Klute, and D. F. Heermann (1976), Hydraulic properties of a porous medium; Measurements and empirical representation, *Soil Sci. Soc. Am. J.*, 40, 203–207.

Hassanizadeh, S. M., and W. G. Gray (1993), Thermodynamic basis of capillary pressure in porous media, *Water Resour. Res.*, 29, 3389–3405, doi:10.1029/93WR01495.

Haverkamp, R., and J.-Y. Parlange (1986), Predicting the water retention curve from particle-size distribution: I. Sandy soils without organic matter, *Soil Sci.*, 142, 325–339, doi:10.1097/00010694-198612000-00001.

Haverkamp, R., M. Vauclin, J. Touma, P. J. Wierenga, and G. Vachaud (1977), A comparison of numerical simulation models for one dimensional infiltration, *Soil Sci. Soc. Am. J.*, 41, 285–294.

Haverkamp, R., M. Vauclin, and G. Vachaud (1984), Error analysis in estimating soil water content from neutron probe measurements: I. Local standpoint, *Soil Sci.*, 137, 78–90, doi:10.1097/00010694-198402000-00002.

Haverkamp, R., J. L. Arrue, and M. Soet (1997), Soil physical properties within the root zone of the vine area of Tomelloso: Local and spatial standpoint, in *Final Integrated Report of EFEDA II (European Field Experiment in a Desertification Area), Spain, CEE Proj. CT920090*, edited by J. F. Santa Olalla, chap. 3, pp. 1–71, Comm. of the Eur. Commun., Brussels.

Haverkamp, R., J. R. Nimmo, and P. Reggiani (2002a), Property-transfer models, in *Methods of Soil Analysis: Part 4. Physical Methods, SSSA Book Ser.*, vol. 5, edited by J. H. Dane and C. G. Topp, pp. 759–782, Soil Sci. Soc. of Am., Madison, Wis.

Haverkamp, R., P. Reggiani, P. J. Ross, and J.-Y. Parlange (2002b), Soil water hysteresis prediction model based on theory and geometric scaling, in *Heat and Mass Transfer in the Natural Environment: A Tribute to J. R. Philip*, edited by D. Smiles et al., pp. 213–246, AGU, Washington, D. C.

Haverkamp, R., F. J. Leij, C. Fuentes, A. Sciortino, and P. J. Ross (2005), Soil water retention: I. Introduction of a shape index, *Soil Sci. Soc. Am. J.*, 69, 1881–1890, doi:10.2136/sssaj2004.0225.

Haverkamp, R., S. Debionne, P. Viallet, R. Angulo-Jaramillo, and D. Decondappa (2006), Movement of moisture in the unsaturated zone, in *Groundwater Engineering Handbook*, 2nd ed., edited by J. W. Delleur, chap. 6, pp. 6.1–6.58, CRC Press, Boca Raton, Fla.

Heinen, M., and P. A. C. Raats (1997), Hysteretic hydraulic properties of a coarse sand horticultural substrate, in *Characterization and Measurement of the Hydraulic Properties of Unsaturated Porous Media I*, edited by M. T. van Genuchten, F. J. Leij, and L. Wu, pp. 467–476, Dep. of Environ. Sci., Univ. of Calif., Riverside, Calif.

Hillel, D. (1980), *Fundamentals of Soil Physics*, Elsevier, New York.

Hoa, N. T., R. Gaudu, and C. Thirriot (1977), Influence of hysteresis effects on transient flows in saturated-unsaturated porous media, *Water Resour. Res.*, 13, 992–996, doi:10.1029/WR013i006p00992.

Hogarth, W. L., J. Hopmans, J.-Y. Parlange, and R. Haverkamp (1988), Application of a simple soil-water hysteresis model, *J. Hydrol.*, 98, 21–29, doi:10.1016/0022-1694(88)90203-X.

Hopmans, J. W., and J. H. Dane (1986), Temperature dependence of soil water retention curves, *Soil Sci. Soc. Am. J.*, 50, 562–567.

Jaynes, D. B. (1992), Estimating hysteresis in the soil-water retention function, in *Indirect Methods for Estimating the Hydraulic Properties of Unsaturated Soils*, edited by M. T. van Genuchten, F. J. Leij, and L. J. Lund, pp. 219–232, Dep. of Environ. Sci., Univ. of Calif., Riverside, Calif.

Kaluarachchi, J. J., and J. C. Parker (1987), Effects of hysteresis with air entrapment on water flow in the unsaturated, *Water Resour. Res.*, 23, 1967–1976, doi:10.1029/WR023i010p01967.

Kool, J. B., and J. C. Parker (1987), Development and evaluation of closed-form expressions for hysteretic soil hydraulic properties, *Water Resour. Res.*, 23, 105–114, doi:10.1029/WR023i001p00105.

Kool, J. B., J. C. Parker, and M. T. van Genuchten (1987), Parameter estimation for unsaturated flow and transport models—A review, *J. Hydrol.*, 91, 255–293, doi:10.1016/0022-1694(87)90207-1.

Kosugi, K. (1994), Three-parameter lognormal distribution model for soil water retention, *Water Resour. Res.*, 30, 891–901, doi:10.1029/93WR02931.

Leij, F. J., W. J. Alves, M. T. van Genuchten, and J. R. Williams (1996), The UNSODA—Unsaturated soil hydraulic database, user's manual version 1.0, *Rep. EPA/600/R-96/095*, Natl. Risk Manage. Res. Lab., Off. of Res. and Dev., U.S. Environ. Prot. Ag., Cincinnati, Ohio.

Leij, F. J., W. B. Russell, and S. M. Lesch (1997), Closed-form expressions for water retention and conductivity data, *Ground Water*, 35, 848–858, doi:10.1111/j.1745-6584.1997.tb00153.x.

Leij, F. J., R. Haverkamp, C. Fuentes, F. Zatarain, and P. J. Ross (2005), Soil water retention: II. Derivation and application of shape index, *Soil Sci. Soc. Am. J.*, 69, 1891–1901, doi:10.2136/sssaj2004.0226.

Libardi, P. L., K. Reichardt, D. R. Nielsen, and J. W. Biggar (1980), Simple field methods for estimating soil hydraulic conductivity, *Soil Sci. Soc. Am. J.*, 44, 3–7.

Liu, Y., J.-Y. Parlange, T. S. Steenhuis, and R. Haverkamp (1995), A soil-water hysteresis model for fingered flow data, *Water Resour. Res.*, 31, 2263–2266, doi:10.1029/95WR01649.

Manzini, G., and S. Ferraris (2004), Mass conservative finite volume methods on 2-D unstructured grids for the Richards' equation, *Adv. Water Resour.*, 27, 1199–1215, doi:10.1016/j.advwatres.2004.08.008.

Mitchel, R. J., and A. S. Mayer (1998), The significance of hysteresis in modeling solute transport in unsaturated porous media, *Soil Sci. Soc. Am. J.*, 62, 1506–1512.

Mualem, Y. (1973), Modified approach to capillary hysteresis based on a similarity hypothesis, *Water Resour. Res.*, 9, 1324–1331, doi:10.1029/WR009i005p01324.

Mualem, Y. (1974), A conceptual model of hysteresis, *Water Resour. Res.*, 10, 514–520, doi:10.1029/WR010i003p00514.

Mualem, Y. (1976), A new model for predicting the hydraulic conductivity of unsaturated porous media, *Water Resour. Res.*, 12, 513–522, doi:10.1029/WR012i003p00513.

Mualem, Y., and E. E. Miller (1979), A hysteresis model based on an explicit domain-dependence function, *Soil Sci. Soc. Am. J.*, 43, 1067–1073.

Nielsen, D. R., M. T. van Genuchten, and J. W. Biggar (1986), Water flow and solute transport processes in the unsaturated zone, *Water Resour. Res.*, 22, 89S–108S, doi:10.1029/WR022i09Sp0089S.

Otten, W., P. A. C. Raats, and P. Kabat (1997), Hydraulic properties of root zone substrates used in greenhouse horticulture, in *Characterization and Measurement of the Hydraulic Properties of Unsaturated Porous Media I*, edited by M. T. van Genuchten, F. J. Leij, and L. Wu, pp. 477–488, Dep. of Environ. Sci., Univ. of Calif., Riverside, Calif.

Parker, J. C., and R. J. Lenhard (1987), A model of hysteretic constitutive relations governing multiphase flow: 1. Saturation-pressure relations, *Water Resour. Res.*, 23, 2187–2196, doi:10.1029/WR023i012p02187.

Parlange, J.-Y. (1976), Capillary hysteresis and relationship between drying and wetting curves, *Water Resour. Res.*, 12, 224–228, doi:10.1029/WR012i002p00224.

Poulovassilis, A. (1962), Hysteresis in pore water and application of the concept of independent domains, *Soil Sci.*, 93, 405–412, doi:10.1097/00010694-196206000-00007.

Rawls, W. J., and D. L. Brakensiek (1985), Prediction of soil water properties for hydrologic modeling, in *Watershed Management in the Eighties*, edited by E. B. Jones and T. J. Ward, pp. 293–299, Am. Soc. of Civ. Eng., Reston, Va.

Richards, L. A. (1931), Capillary conduction of liquids through porous media, *Physics*, *1*, 318–333, doi:10.1063/1.1745010.

Rogowski, A. S. (1971), Watershed physics: Model of soil moisture characteristics, *Water Resour. Res.*, *7*, 1575–1582, doi:10.1029/WR007i006p01575.

Russo, D., W. A. Jury, and G. L. Butters (1989), Numerical analysis of solute transport during transient irrigation: 1. The effect of hysteresis and profile heterogeneity, *Water Resour. Res.*, *25*, 2109–2118, doi:10.1029/WR025i010p02109.

Schaap, M. G., and F. J. Leij (1998), Database-related accuracy and uncertainty of pedotransfer functions, *Soil Sci.*, *163*, 765–779, doi:10.1097/00010694-199810000-00001.

Schaap, M. G., F. J. Leij, and M. T. Van Genuchten (1998), Neural network analysis for hierarchical prediction of soil hydraulic properties, *Soil Sci. Soc. Am. J.*, *62*, 847–855.

Scott, P. S., G. J. Farquhar, and N. Kouwen (1983), Hysteretic effects on net infiltration, in *Advances in Infiltration*, *Publ. 11i83*, pp. 163–170, Am. Soc. of Agric. Biol. Eng., St. Joseph, Mich.

Si, B. C., and R. G. Kachanoski (2000), Unified solution for infiltration and drainage with hysteresis: Theory and field test, *Soil Sci. Soc. Am. J.*, *64*, 30–36.

Sinclair, D. F., and J. Williams (1979), Components of variance involved in estimating soil water content and water content change using a neutron moisture meter, *Aust. J. Soil Res.*, *17*, 237–247, doi:10.1071/SR9790237.

Natural Resources Conservation Service (NRCS) (1960), *Soil Classification System, 7th Approximation*, U.S. Dep. of Agric., Gov. Print. Off., Washington, D. C.

Topp, G. C. (1971), Soil-water hysteresis: The domain theory extended to pore interaction conditions, *Soil Sci. Soc. Am. J.*, *35*, 219–225.

Vachaud, G., M. Vauclin, and J. Colombani (1981), Bilan hydrique dans le Sud-Tunisien, *J. Hydrol.*, *49*, 31–52, doi:10.1016/0022-1694(81)90204-3.

van Genuchten, M. T. (1980), A closed form equation for predicting the hydraulic conductivity of unsaturated soils, *Soil Sci. Soc. Am. J.*, *44*, 892–898.

van Genuchten, M. T., F. J. Leij, and S. R. Yates (1991), The RETC code for quantifying the hydraulic functions of unsaturated soils, *Rep. EPA/600/2-91/065*, U.S. Environ. Prot. Ag., Washington, D. C.

Vereecken, H. (1992), Derivation and validation of pedotransfer functions for soil hydraulic properties, in *Indirect Methods for Estimating the Hydraulic Properties of Unsaturated Soils*, edited by M. T. van Genuchten, F. J. Leij, and L. J. Lund, pp. 473–488, Dep. of Environ. Sci., Univ. of Calif., Riverside, Calif.

Viaene, P., H. Vereecken, J. Diels, and J. Feyen (1994), A statistical analysis of six hysteresis models for the moisture retention characteristic, *Soil Sci.*, *157*, 345–355, doi:10.1097/00010694-199406000-00003.

Whitmore, A. P., and M. Heinen (1999), The effect of hysteresis on microbial activity in computer simulation models, *Soil Sci. Soc. Am. J.*, *63*, 1101–1105.

————————————

D. Canone, S. Ferraris, and R. Haverkamp, Department of Economics and Agricultural, Forestry and Environmental Engineering, University of Turin, via Leonardo da Vinci 44, I-10095 Grugliasco, Italy. (randel@hmg.inpg.fr)

G. Sander, Department of Civil and Building Engineering, Loughborough University, Loughborough LE11 3TU, UK.